Stratum Corneum Protein Dynamics as Evaluated by a Spin-Label Maleimide Derivative: Effect of Urea

Antonio Alonso,* Wilmar Pereira dos Santos,* Sérgio Jacintho Leonor,* Judes Gonçalves dos Santos,* and Marcel Tabak†

*Instituto de Física, Universidade Federal de Goiás, Goiânia 74001-970, Brazil; and †Instituto de Química de São Carlos, Universidade de São Paulo, São Carlos 13560-970, Brazil

ABSTRACT The stratum corneum (SC) protein dynamics in the sulfhydryl group regions was studied by electron paramagnetic resonance (EPR) spectroscopy of a covalently attached maleimide derivative spin label. A two-state model for the nitroxide described the coexistence of two spectral components in the EPR spectra. The so-called strongly immobilized component arises from a spin-label fraction with the nitroxide moiety hydrogen-bonded to protein (rigid structure) and the weakly immobilized component is provided by the spin labels with higher mobility (~10 times greater) exposed to the aqueous environment. The relative populations between these two states are in thermodynamic equilibrium. The apparent energetic gain for the nitroxide to form a hydrogen bond with the backbone rather than to be dissolved in the local environment was ~10 kcal/mol in the temperature range of 2–30°C and ~6 kcal/mol in the range of 30–70°C. Urea treatment caused a drastic increase in the segmental motion of the polypeptide chains that was completely reversible by its removal. Our analyses also indicated that the urea induced unfolding of the SC proteins opening the thiol group cavities. This work can also be useful to improve the spectral analysis of site-directed spin-labeling, especially for a more quantitative description of the nitroxide side chain mobility.

INTRODUCTION

The outermost ~10-μm-thick layer of the mammalian skin, the stratum corneum (SC), plays an important role as a low-permeability membrane that controls transepidermal water loss and the permeation of other substances in both directions across skin. Essential for terrestrial life, the SC consists of an array of 10–20 layers of flat, polygonal cells, the keratin-filled corneocytes, embedded in a matrix of lamellar lipids (Breathnach et al., 1973; Swartzendruber et al., 1989; Wertz et al., 1989) that consist essentially of ceramides, cholesterol, and saturated fatty acids (Gray et al., 1982). Corneocytes are terminally differentiated keratinocytes containing a cornified cell envelope on the cytoplasmic face of the plasma membrane. The cell envelope is a 10–20-nm-thick protein assembly, highly insoluble due to extensive cross-linking of intermolecular disulfide bonds (Matoltsy and Matoltsy, 1970) and N^{ϵ}-(γ-glutamyl)lysine isopeptide bonds, which is formed by the action of transglutaminase present in the keratinocyte membrane (Abernethy et al., 1977; Rice and Green, 1977; Goldsmith et al., 1974).

The high insolubility of the cornified cell envelope has precluded the use of direct methods to examine its proteins (Steven and Steinert, 1994). Nevertheless, mathematical modeling comparing the amino acid compositions of purified cell envelope and those from precursor proteins to the cell envelope had indicated a loricrin content of 65–70% in human and 80–85% in mouse, with smaller amounts of filagrin, cysteine-rich protein, involucrin, small proline-rich proteins and cistatin α (Steven and Steinert, 1994; Steinert and Marekov, 1995), among other cell junctional proteins (Steinert and Marekov, 1999). On the outer surface of the cell envelope there is a monolayer of ω-hydroxyceramides, covalently linked by an ester bond, forming the corneocyte lipid envelope (Wertz and Downing, 1987; Swartzendruber et al., 1989; Wertz et al., 1989; Behne et al., 2000). Recent data have suggested that transglutaminase 1 can also catalyze the esterification of these ceramides and that they are bound most abundantly to involucrin (Nemes et al., 1999) which, being located next to the plasma membrane, is one of the first proteins to initiate the cell envelope assembly (Steinert and Marekov, 1999). One interesting idea about the lipid-protein interactions in SC is that the protein-bonded ceramides interdigitate with intercellular lipids, forming a scaffold for the organization and stability of the intercellular lamellae (Hohl, 1990; Downing, 1992; Nemes et al., 1999).

In previous works (Alonso et al., 1995, 1996) we have studied the lipid chain dynamics in SC through electron paramagnetic resonance (EPR) spectroscopy of fatty acid-derivative spin labels incorporated directly into SC-lipid domains of the intact tissue. The SC-lipid fluidity increases with tissue water content as well as increases the water diffusion coefficient (El-Shime and Princen, 1978; Blank et al., 1984, Alonso et al., 1996), suggesting that there are mechanisms in SC to control the permeability leading to a greater transepidermal water loss when a water excess in the skin occurs. However, it is expected that water also increases protein mobility, raising an important issue to un-

Received for publication 12 January 2001 and in final form 23 August 2001.

Address reprint requests to Dr. Antonio Alonso, Universidade Federal de Goiás, Goiânia 74001-970, Brazil. Tel.: 55-62-521-1470; Fax: 55-62-521-1014; E-mail: alonso@fisufg.br.

© 2001 by the Biophysical Society

0006-3495/01/12/3566/11 $2.00

derstand whether the cell envelope can affect or modulate the extracellular lipid organization. More recently (Alonso et al., 2000a) we have compared the lipid chain dynamics in three types of SC samples: intact SC, lipid-depleted SC (containing only the lipids from the cell lipid envelope covalently attached to proteins), and dispersion of SC-extracted lipids. The EPR spectra indicated very different mobility states for the three samples with the following relation of rigidity: lipid dispersion $<$ intact SC $<$ cell envelope lipids, suggesting that lipid-protein interactions in SC are important and that the intact cell lipid envelope (with unbound lipids structured together with the covalently bonded ones) can provide the major physical barrier in the skin due to its low mobility state.

EPR spectroscopy of maleimide-derivative spin labels has been largely used to assess mobility and conformational changes at sulfhydryl groups of proteins (Esmann et al., 1987; Sankarapandi et al., 1995; Liu and Zhou, 1995) and to study the overall rotational diffusion of the membrane proteins through saturation transfer EPR (Esmann et al., 1989, 1992). More recently, the method of site-directed spin labeling is emerging as a new tool to analyze structure and conformational dynamics of proteins (Mchaourab et al., 1999). In this approach a single cysteine residue is introduced by mutagenesis at a predetermined position in a protein sequence, substituting the corresponding amino acid, and subsequently modified with a thiol-specific spin label, generally a methanethiosulfonate derivative (Mchaourab et al., 1996). The nitroxide side chain accessibility, the side chain dynamics, and the estimates of the distances between two-engineered cysteine residues are addressed by EPR (Zhan et al., 1995; Mchaourab et al., 1999; Russell et al., 1999).

The EPR spectra of spin-labeled polypeptide chains are generally characterized by the coexistence of two spectral components with very different states of probe mobility. These components are commonly called strongly and weakly immobilized ones, and are associated with restricted and less restricted motion on the 9.4 GHz EPR time scale for nitroxide motion; however, as has been pointed out by Barnes and co-workers (1999), the origin of the two states remains a matter for speculation. Very recently, we have presented (Alonso et al., 2000b) a new interpretation for the origin of these two-component EPR signals, associated with different hydrogen bond formations in the vicinity of the protein thiol group. We also have shown that SC protein mobility essentially did not change after exhaustive lipid extraction with organic solvents; only small alterations were observed and explained by a larger opening of the sulfhydryl pocket upon the delipidization process. Here, we present new evidence that corroborates our interpretation of the EPR spectra of nitroxides linked to proteins, through the analysis by spectral simulation of the dynamic and conformational changes caused by the treatment of SC with urea. We hope that our results can contribute to increase the EPR-application potential to study protein dynamics, and in the case of SC proteins, contribute new data regarding the protein participation in the SC function as a permeability controller.

MATERIALS AND METHODS

Preparation of SC

The SC membranes were obtained from newborn Wistar rats aged less than 24 h and prepared as described previously (Alonso et al., 1995, 2000b). After sacrifice, the skin was excised and fat was removed by rubbing in distilled water. The skin was allowed to stand for 5 min in a desiccator containing 0.5 l anhydrous ammonium hydroxide and allowed to float in distilled water with the epidermal side in contact with the water. After 2 h the SC was removed to a filter paper and transferred to a Teflon-coated screen, washed with distilled water, and allowed to dry in ambient conditions. The membranes were stocked with 1 l silica gel in a desiccator under a moderate vacuum.

Maleimide-spin-labeling of stratum corneum and albumin

The spin-label maleimide-nitroxide derivative 3-maleimido-1-oxyl-2,2,6,6-tetramethylpyrrolidine (5-MSL) was purchased from Aldrich Chemical Co. (Milwaukee, WI). Spin-labeling and measurements were performed at pH 5.1, approximately the pH found at the skin surface (Öhman and Vahlquist, 1998). An intact piece of SC ($\sim$1 mg) was incubated for 30 min at 24°C in acetate-buffered saline (ABS) (10 mM acetate, 150 mM NaCl, and 10 mM EDTA), pH 5.1, followed by a second incubation of 15 min in the buffer with 2 mM spin label. The SC membrane was dried on filter paper and incubated in $\sim$2 ml buffer under moderate agitation for 2 min, in each of five successive washings aiming to eliminate free unbound label. The sample was introduced into a capillary tube for EPR measurements, having a water content estimated by gravimetric measurements as 58 $\pm$ 7% (w/w). Under these conditions the SC was considered to be in a fully hydrated state. Treatments with urea were performed incubating the spin-labeled SC for 1 h at fixed urea concentrations in buffer. Serum bovine albumin (Sigma Chemical Co., St. Louis, MO) at 0.2 mM was incubated at $\sim$4°C for 24 h in phosphate-buffered saline (10 mM phosphate, 150 mM NaCl, and 10 mM EDTA, pH 7.4) with 1 mM 5-MSL. To remove the free spin label the albumin was dialyzed for $\sim$24 h at $\sim$4°C against the phosphate-buffered saline.

EPR spectroscopy

A Bruker ESP 300 spectrometer equipped with the ER 4102 ST resonator and operating at X-band (9.4 GHz) was utilized in our investigations. The spectral parameters were as follows: microwave power, 20 mW; modulation frequency, 100 KHz; modulation amplitude, 1.024 G; magnetic field scan, 100 G; sweep time, 168 s and detector time constant, 41 ms. Temperature was controlled within 0.3°C by the nitrogen stream system (Bruker, Rheinstetten, Germany). EPR spectra simulations were performed by nonlinear least-squares (NLLS) fits, using the general slow-motional program (Schneider and Freed, 1989; Budil et al., 1996). This program permits the fitting of a single spectrum with two components having different mobility and magnetic tensor parameters. The magnetic **g** and **A** tensors are defined in a molecule-fixed frame, where the constants of rotational diffusion rates around the x, y, and z axis are included (Budil et al., 1996). By convention, the x axis points along the N–O bond, the z axis is parallel to the 2 pz axis of the nitrogen atom, and the y axis is perpendicular to x and z (Schneider and Freed, 1989). The parameters of tensors **g** and **A** (G) used in the spectral calculations for components 1 and

2, here called S and W components, respectively, were: g_{xx}(S) = 2.0098, g_{yy}(S) = 2.006, g_{zz}(S) = 2.002, g_{xx}(W) = 2.0079, g_{yy}(W) = 2.0054, g_{zz}(W) = 2.003, a_{xx}(S) = 6.9, a_{yy}(S) = 7.9, a_{zz}(S) = 36.2, a_{xx}(W) = a_{yy}(W) = 7.5, a_{zz}(W) = 36.2. The linewidth tensor was fixed to $w_{xx} = w_{zz} = 0.3$ and $w_{yy} = 2.0$ G for the two components. These parameters were determined by a general analysis of the overall spectra from this work and, once determined, all EPR spectra were simulated using the same prefixed values.

The a_{zz} and g_{zz} parameters for the immobilized component were measured directly in the spectra at −150°C. The inferred position of the central resonance line and the isotropic hyperfine splitting a_0 of the more mobile component gives the averages of the principal values of **g** and **A** tensors. The other tensor components were adjusted to obtain a better convergence of the fittings and the quality of the simulations was very sensitive to these magnetic parameters, especially to those from the near-rigid limit EPR spectra. To reduce the number of parameters and to simplify the simulation, we have considered the two components as having isotropic motion (a spherical form was assumed for **R** tensors, $\mathbf{R}_{bar}$S and R_{bar}W).

RESULTS

Interpretation of EPR spectra of spin-labeled proteins

Shown in Fig. 1 *a* is the EPR spectrum at 38°C of maleimide spin label 5-MSL covalently bound to the SH groups of the SC. The EPR spectra of spin-labeled proteins are composed, in general, of basically two spectral components, indicating the coexistence of two spin-probe populations with very different mobility states. By simulation it is possible to separate the two spectral components that overlap in the composed spectrum. The normally called strongly (Fig. 1 *b*) and weakly (Fig. 1 *c*) immobilized components are denoted as S and W components, respectively. In Fig. 1 *d* the total simulated spectrum is shown together with the experimental one. The less mobile component on the 9.4 GHz EPR time scale for nitroxide radicals represents a large fraction of the spectrum and permits measurement of the outer hyperfine extrema, the parameter $2T'_{//}$, which reflects the probe mobility. The more mobile component W presents three sharp resonance lines having an isotropic hyperfine splitting $2a_0$, which is very sensitive to the solvent polarity where the nitroxide moiety is dissolved. Polarity of the solvent tends to increase the unpaired electron spin density on the nitrogen nuclei and, thus, increase the hyperfine splitting. This increase occurs mainly when the oxygen atom of the nitroxide radical can form hydrogen bonds, as occurs in aqueous systems. The apparent hyperfine coupling, $2a_0$, of the weakly immobilized component W is the same as that observed for the EPR spectrum of 5-MSL in buffer (17.1 ± 0.5 G, spectrum not shown), indicating that the nitroxides in the W component are all exposed to water (hydrophilic environment).

The method of Griffith and Jost (1976) can be used to examine whether the nitroxides that contribute to the strongly immobilized component are forming a hydrogen bond with some site of the lateral chains of the proteins. In the motionally frozen state the parameter $2T'_{//}$, of the 9.4 GHz EPR spectra, gives $2A_{zz}$, the *z*-component of the hyperfine tensor. When the nitroxide radical is frozen in a hydrophobic region, the expected $2A_{zz}$ value is 65.0 ± 0.5 G, which will be the value for the non-hydrogen-bonded N–O group. At 38°C the $2T'_{//}$ value is 66.0 ± 0.5 G (Fig. 1 *a*) and tends to 72.4 ± 0.5 G at −70°C, indicating the presence of hydrogen bond with the oxygen atom of the nitroxide moiety. This result shows that the spin labels that contribute to the so-called strongly immobilized component are strongly attached to proteins. From one side the maleimide ring is covalently bond to the sulfur atom of the protein, and from the other side the N–O fragment is hydrogen-bonded to some amide or lateral chains of the residues (rigid structure).

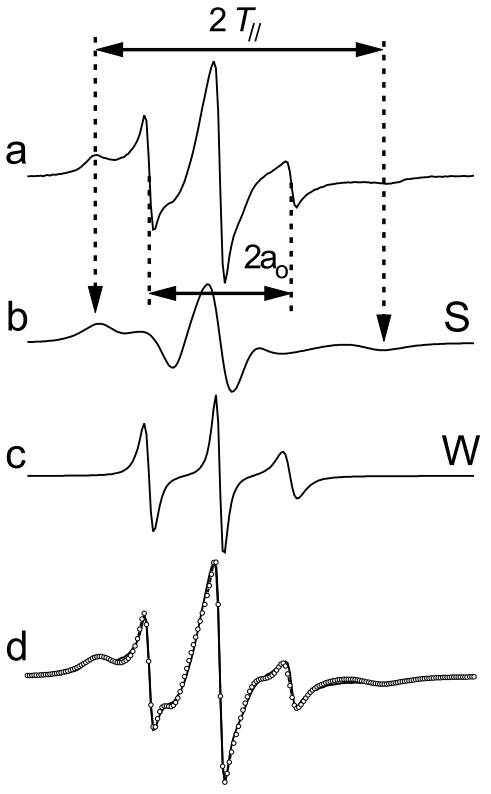

FIGURE 1 Experimental and simulated EPR spectra at 38°C of maleimide spin label 5-MSL covalently bound to sulfhydryl groups of the stratum corneum in ABS pH 5.1. (*a*) Experimental spectrum. The best-fit spectra were obtained by NLLS fit, considering two components for all fits. (*b* and *c*) Calculated strongly (S) and weakly (W) immobilized components, respectively. (*d*) Experimental (*line*) and simulated (*open circles*) spectra. The EPR parameters $2T'_{//}$, the outer hyperfine splitting, and $2a_0$, the isotropic hyperfine splitting are indicated. Total magnetic field scan: 100 G.

The population ratio of the strongly and weakly immobilized components, N_S/N_W, in the composed spectrum reduces with the increase of the temperature. This effect is completely reversible, showing that the two components are in a thermodynamic equilibrium. The results mentioned above suggest that these two spectral components arise from

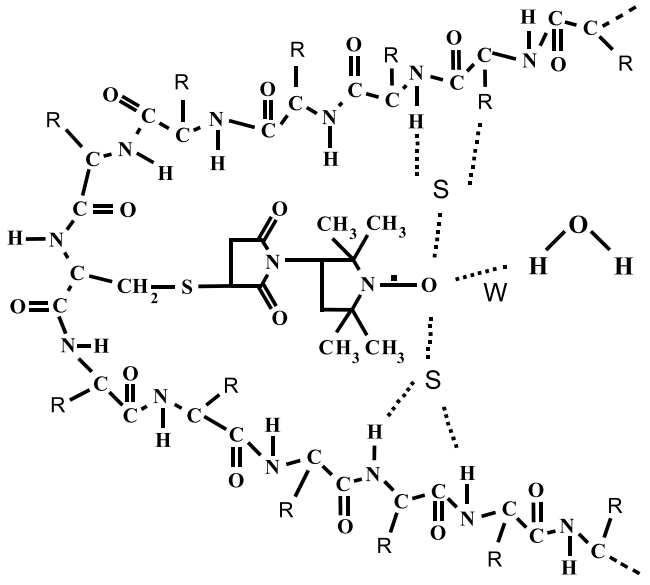

FIGURE 2 Schematic molecular model illustrating the spin label 5-MSL bound to the polypeptide chain in the sulfhydryl group region. The nitroxide moiety can form hydrogen bonds either with the amino acid residue or peptidic amide hydrogen, generating the strongly immobilized component (S), or with the water to generate the weakly immobilized component (W). The side chains from amino acid residues are not shown for simplicity.

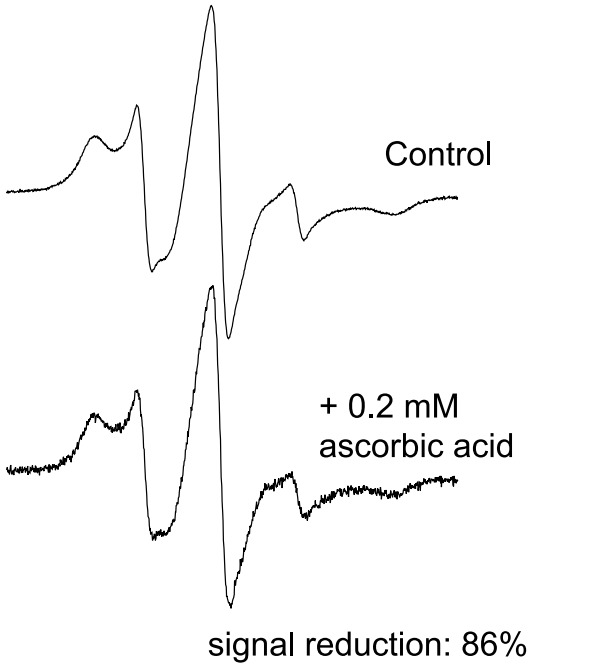

FIGURE 3 EPR spectra at 30°C of maleimide spin label 5-MSL covalently bound to SH groups of the stratum corneum in ABS pH 5.1 before (*top*) and after (*bottom*) nitroxide reduction by ascorbic acid. The signal reduction was 86% after 5 min of incubation with 0.2 mM ascorbic acid; the spectral line shape essentially did not change. The magnetic field scan width is 100 G.

two interchangeable nitroxide states: hydrogen-bonded (S) and non-hydrogen-bonded (W) to protein. In Fig. 2 a model illustrating the accommodation of 5-MSL in the sulfhydryl cavity is presented. Thus, when the nitroxide is hydrogen-bonded to a protein site its motions reflect essentially the segmental motions of the backbone relative to the average protein structure. This type of motion produces the less mobile EPR spectral line shape, the S signal (Fig. 1 *b*). When the nitroxide moiety is non-hydrogen-bonded to protein, its motions are related to the effective correlation time due to rotational isomerizations around the bonds that link the nitroxide ring to the protein. This other type of motion appears as the more mobile component in the EPR spectra, the W signal (Fig. 1 *c*).

To test the above interpretation, which is very important for the EPR analysis of proteins in general, three experiments were performed: 1) nitroxide reduction with ascorbic acid did not change the shape of the spectrum, as can be seen in Fig. 3. As the reducer agent reaches the nitroxide moiety via the aqueous phase and because the labels from the S component are contacting the protein, it will be expected that the reduction takes place for the W component population. However, because a proportional reduction for the two components was observed, the experimental result is consistent with the idea that the same nitroxide contributes to the two components and that the conversion rate between the two states, S and W, is faster than the reduction rate, maintaining the observed equilibrium between these two states. 2) In spin-labeled albumin, used as a simple protein model, it was possible to record EPR spectra under several nitroxide reduction rates by varying the ascorbate concentration. In Fig. 4 EPR spectra are shown for three reduction rates. For nitroxide reduction with a half-life time of 16.5 min, the line shape was kept the same as that for the original sample without reductant, and for half-life times of 7.9 and 5.3 min the W component was reduced first, indicating that the mean lifetime of the spin labels in the W component is between 16.5 and 7.9 min at 26°C. 3) The water-soluble paramagnetic relaxation agent nickel II was introduced in the SC samples to verify its accessibility to the S and W components. The EPR signal tends to disappear as the nitroxide undergoes collisions with the line-broadening agent. Adding 250 mM $NiCl_2$ to the SC sample eliminates the weakly immobilized component from the EPR spectrum of 5-MSL, whereas the strongly immobilized one remains essentially unchanged (Fig. 5). We believe that when the nitroxide is hydrogen-bonded to the protein (S component) it is less exposed to the solvent and to the nickel II, consequently.

Urea increases the SC protein mobility

In Fig. 6 the experimental and simulated EPR spectra at several temperatures of 5-MSL bound to SC sample are shown, without treatment (Fig. 6 *A*) and treated with 8 M

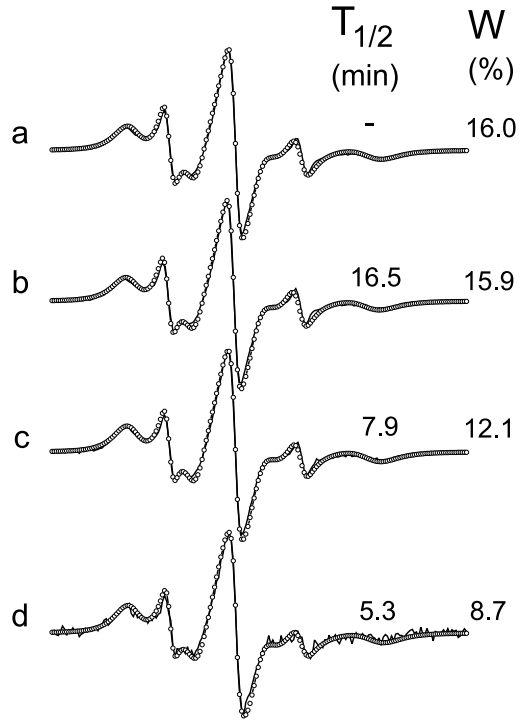

FIGURE 4 Experimental (*line*) and simulated (*open circles*) EPR spectra at 25°C of spin label 5-MSL bound to the sulfhydryl group of bovine serum albumin. (*a*) Control, without nitroxide reduction by ascorbate. The percentage of weakly immobilized component (W) in the spectrum was 16.0%. Under nitroxide reduction the EPR spectra did not change for a half-lifetime ($T_{1/2}$) of 16.5 min (*b*) but have a smaller contribution of the W component for half-lifetimes of 7.9 and 5.3 min (spectra *c* and *d*). The magnetic field scan width is 100 G. From top to bottom the used concentrations of ascorbic acid and the EPR signal intensities were, respectively, 0, 5, 9, and 11 mM and 100, 70, 36, and 6%.

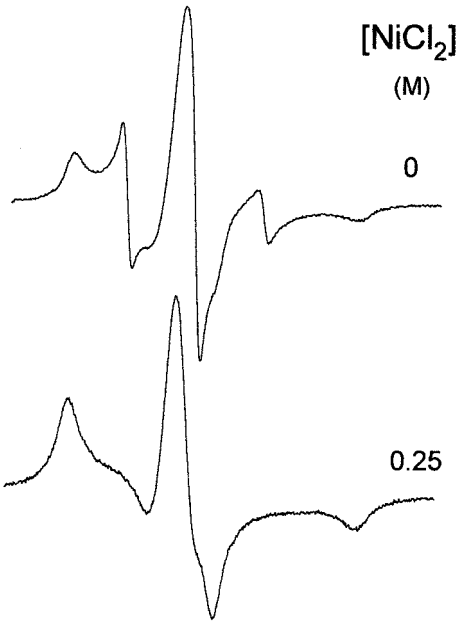

FIGURE 5 EPR spectra at 34°C of 5-MSL in stratum corneum (pH 5.1) without (*top*) and with (*bottom*) the presence of a paramagnetic relaxing agent. The EPR signal tends to disappear with the increase in the collision frequency between the nitroxide and the nickel ions. The nickel ions reach the spin labels from component W more easily. Range of magnetic field scans: 100 G.

urea (Fig. 6 *B*). The fitting convergence was not very good only for the SC sample without treatment and at lower temperatures. For each spectral simulation the relative populations of the two fractions of radicals and the rotational correlation parameters $\mathbf{R}_{bar}$S (component S) and $\mathbf{R}_{bar}$W (component W) can be obtained (Budil et al., 1996).

In Fig. 7 the population ratio of the spin labels in the two motional states is presented as a function of the reciprocal temperature. In the plot for non-treated SC a linear and biphasic behavior is apparent with higher change rates of N_S/N_W ratio in the temperature range from 2 to 26°C than in the range of 26–70°C. The treatment with 8 M urea leads to a large reduction in the N_S/N_W ratio, with a single smaller slope apparent in the plot. It is also noteworthy that all EPR spectra were completely reversible. Even in the case of urea-treated samples, after measurements up to 70°C the samples were measured again at 38°C, and no significant changes were observed (Fig. 7). Considering that the relation of spin-label populations is given by the Boltzmann distribution, we have:

$$N_S/N_W = A \exp(E_a/RT) \quad (1)$$

or

$$\log N_S/N_W = \log A + E_a/(2.302RT) \quad (2)$$

where A is a pre-exponential factor that reflects the ratio between the number of sites for S and W ($A = N_{S0}/N_{W0}$) and E_a is the apparent activation energy. Equation 2 shows that, in practice, the numerical values of E_a can be determined from the slope coefficient of a plot such as the one presented in Fig. 7. In Table 1 the apparent activation energies calculated for these curves are presented. The activation energy is the energy required to dissociate the motionally restricted nitroxide moiety from the protein. In other words, it represents the energetic gain of 5-MSL to form a hydrogen bond with the protein rather than to be exposed to the buffer. The urea-treated sample showed a lower value for the N_S/N_W ratio in the whole temperature range, which may be associated with the pre-exponential factor that should reflect the ratio between the sites for S and W components (the SH groups are probably more exposed to water in the urea-treated SC or the presence of urea prevents the hydrogen-bonding of the nitroxide to the protein). The significant conformational changes caused by urea in the SC proteins are also reflected in a reduction in the activation energy.

In Fig. 8 the parameters obtained from the simulations are presented for the strongly immobilized (Fig. 8 *A*) and weakly immobilized (Fig. 8 *B*) radicals as a function of the

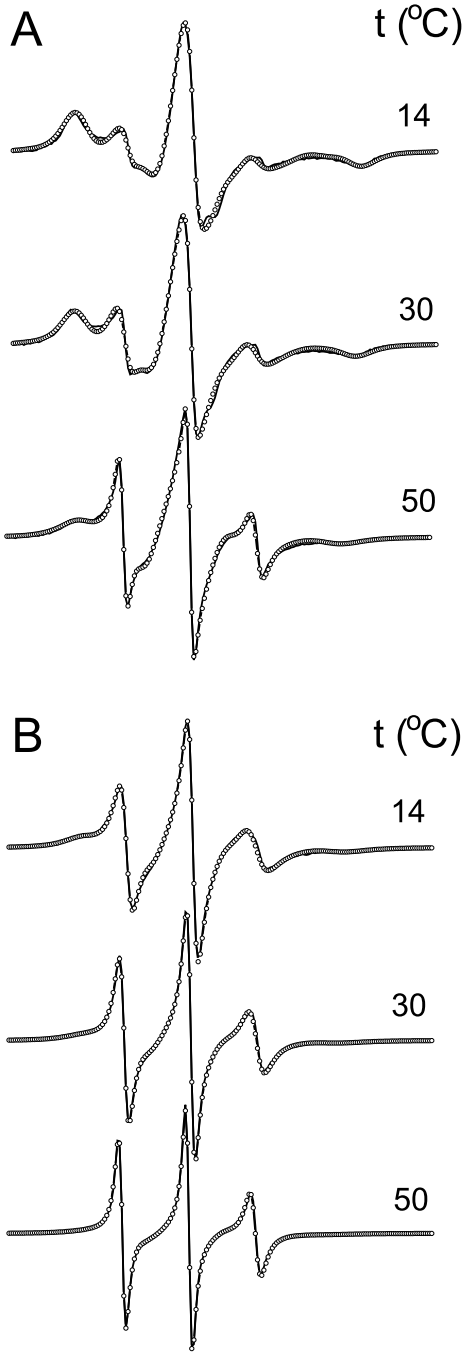

FIGURE 6 Experimental (*line*) and best-fit (*open circles*) EPR spectra of 5-MSL in stratum corneum (pH 5.1) at several temperatures. (*A*) Stratum corneum without treatment; (*B*) stratum corneum treated with 8 M urea. Range of magnetic field scans: 100 G.

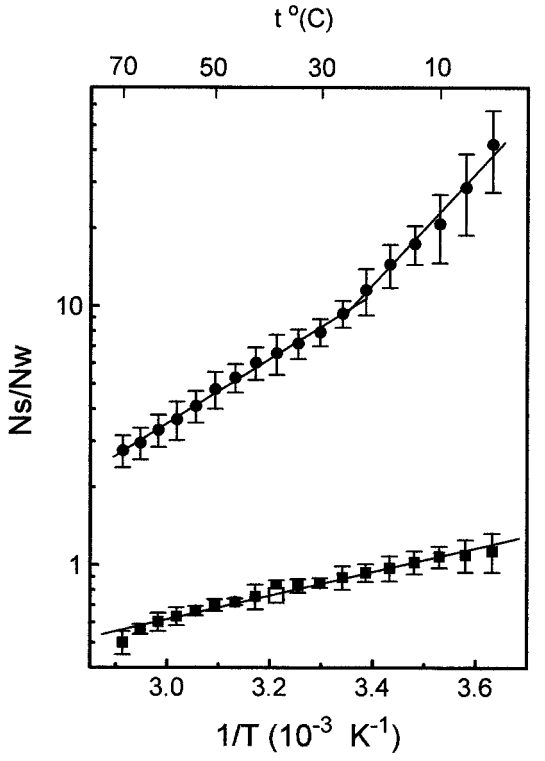

FIGURE 7 The population ratio of the strongly and weakly immobilized components, N_S/N_W, in the EPR spectra of stratum corneum labeled with 5-MSL (pH 5.1), as a function of the reciprocal absolute temperature. The symbols refer to stratum corneum without treatment (*circles*) and treated with 8 M urea (*squares*); the open square corresponds to the value obtained for the sample with urea after the measurement up to 70°C, and lowering the temperature back to 38°C.

reciprocal absolute temperature. It is seen that the parameter $\mathbf{R}_{bar}$S is very sensitive to temperature and that urea causes a significant increase in the backbone protein mobility in the entire temperature range. The parameter $\mathbf{R}_{bar}$W, which reflects the nitroxide mobility within the SH-group cavity, shows an atypical behavior at low temperatures for native SC, having a decrease in the range from 2 to ~26°C, followed by an increase at temperatures above ~26°C. For urea-treated samples the cavity effects are not apparent, showing a linear behavior and suggesting that urea increases the cavity opening of the sulfhydryl groups particularly at lower temperatures.

Because the spin labels from the S component are "tethered" in the protein, they reflect the segmental motion of the backbone and, thus, the parameter $2T'_{//}$ can be used to characterize local protein mobility. In Fig. 9 we present the dependence of $2T'_{//}$ with the urea concentration. Urea

TABLE 1 Activation energy for exchange between the motional restricted and the mobile components in EPR spectra of stratum corneum labeled on SH groups with the maleimide spin label 5-MSL

Stratum Corneum Sample	Temperature Range (°C)	ΔE (kcal/mol)*
Control	2–26	9.9 ± 1.7
	26–70	5.7 ± 0.2
8 M Urea	2–70	2.1 ± 0.4

*The numerical values of E_a were calculated using Eq. 2 and the slope coefficient of the plots as the one presented in Fig. 7. See text for details.

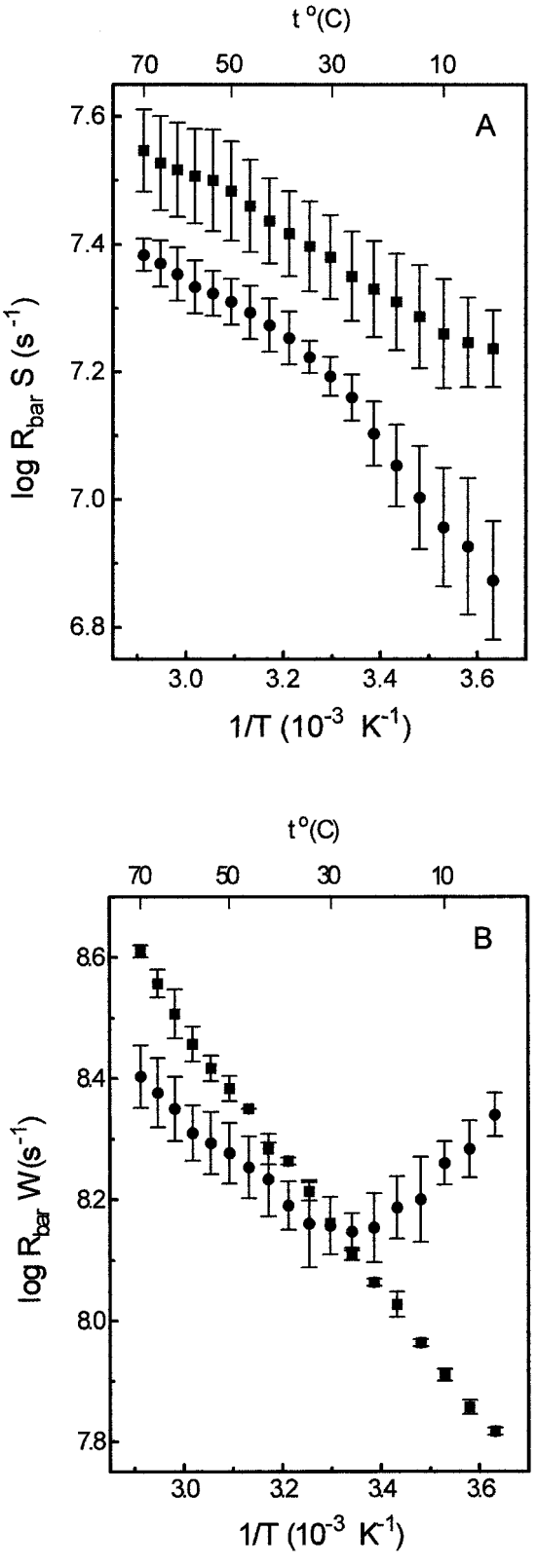

FIGURE 8 Rotational diffusion parameters $R_{bar}S$ (*A*) for the strongly immobilized component and $R_{bar}W$ (*B*) for the weakly immobilized component, obtained from the spectral fitting of 5-MSL EPR spectrum in stratum corneum (pH 5.1). The symbols refer to stratum corneum without treatment (*circles*) and treated with 8 M urea (*squares*).

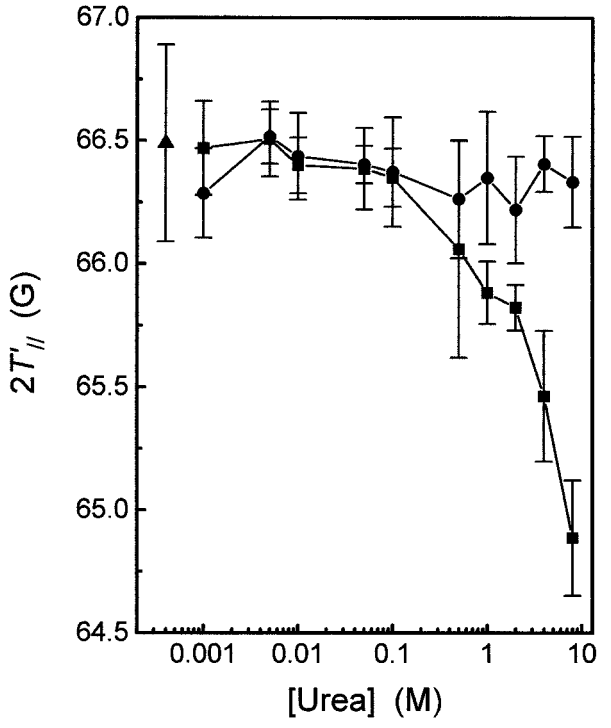

FIGURE 9 EPR parameter $2T'$, the outer hyperfine spitting (see Fig. 1) of 5-MSL covalently bound to sulfhydryl groups of stratum corneum (pH 5.1) as a function of urea concentration in the buffer (*squares*). After each mesurement the sample was washed with buffer to remove urea, and re-measured (*circles*). The triangle corresponds to control sample in the absence of urea.

caused a significant increase in the protein mobility at 1 M, and this effect grew up to 8 M. Each sample was washed to remove the urea after the measurement, and re-measured. It is seen that the urea effect was completely reversible because, after washing, the result was the same as in the absence of urea.

DISCUSSION

EPR spectroscopy of nitroxide-labeled proteins

A thermodynamic equilibrium between the main components of EPR spectra of nitroxide attached to proteins was observed with relatively high apparent activation energies. These calculated energies are only apparent because we have supposed that the pre-exponential factor (N_{S0}/N_{W0}, Eq. 2) does not change with the temperature, assuming a linear behavior in the plots from Fig. 7. Although the behavior of the sample treated with urea does seem to be linear in the whole temperature range, in the case of the control sample it was arbitrarily assumed to be linear, with different slopes for the two temperature intervals. Particularly for the control sample at temperatures below 30°C, an increase of the W-sites number could occur with the increase in temperature because the proteins could undergo conformational

changes where the SH groups become more exposed to the solvent. It is conceivable that for the samples treated with urea the solvent-exposition degree of the SH groups is quite great in all the temperature range and, in this case, the calculated activation energy reflects the actual energy required for hydrogen bond formation between the nitroxide moiety and the protein. We believe that this is also the case for the control sample above 30°C; that is, for this temperature range the solvent-exposition degree practically does not change and the calculated energy actually reflects the energy gap between the two states.

It is remarkable that our spectral fittings were not so good for the control sample below 30°C and that the convergence was better when we considered an anisotropic rotational motion for the nitroxide with low motion around the *y*-direction (perpendicular to the N–O bond and the $2p\pi$ orbital), as was made in a previous work (Alonso et al., 2000b). However, this alteration does not change in an essential way the results presented here. Thus, our determination of E_a for temperatures between 2 and 26°C are not very accurate. Although we believe strongly that the slope is larger in this temperature range than between 26 and 70°C, we did not rule out the possibility that some other model for the nitroxide motion will lead to better fittings of the experimental spectra and to a small difference in this result. For bovine serum albumin the simulation is easier than for SC, where the nitroxide motion is slower. The EPR spectrum for albumin at 25°C (Fig. 4) is similar to the spectrum for SC at 38°C (Fig. 1), which also was easy to simulate. It is important to notice that while albumin is tumbling in solution the SC proteins are in the tissue, with many disulfide and isodipeptide cross-links among them.

It is interesting that maleimide derivative probes with different chain lengths between the maleimide group and the nitroxide ring have been used to estimate the depth of the sulfhydryl pocket in rhodopsin (Delmelle and Virmaux, 1977) and plasma fibronectin (Lai et al., 1984). For probe lengths of 12.9 Å or greater the strongly immobilized component goes to a minimum in the spectrum when the nitroxide is outside the sulfhydryl pocket. This result is consistent with a low number of available local protein sites able to form hydrogen bonds relative to the number of sites able to form hydrogen bonds to the solvent (small pre-exponential factor, eq. 2). In the case of site-directed spin labeling a multiplicity of situations can occur and the analysis becomes quite complex, but it would be expected that the proportion of the S component in the spectral line shape would be greater in several circumstances: 1) smaller nitroxide side chains, 2) less-hydrophilic local environments, 3) more rigid backbones, and 4) more buried protein SH groups. The methodology and the present interpretation can also be applied to DNA study. Liang and co-workers (2000) have tested four spin labels with different probe lengths bound to DNA oligomers of three lengths and a polymer. The authors have found EPR spectra with two components for the polymer with the smaller probe length. The double component formation is dependent on a rigid structure to interact with the spin probe (the rotational tumbling of the polymer is the lower one) and the probability of the S component formation should increase with the decrease of the probe length. For the existence of these two distinct spectral components, any exchange rate between them must be slower than the EPR time scale (Liang et al., 2000). As can be observed in Fig. 4, this exchange rate is very low.

In the site-directed spin-labeling method it is usual to calculate an "accessibility parameter" from the power saturation behavior of the nitroxide in the presence of polar (NiAA and NiEDDA) and apolar (O_2) paramagnetic reagents (Zhan et al., 1995; Russell et al., 1999). Because the fast-relaxation effects on the nitroxide EPR signal are proportional to the collision frequency of nitroxides with the paramagnetic species, the estimated accessibility heavily weights the W component, because during the time that the nitroxide is hydrogen-bonded to the protein (generating the S component) it is much less accessible to the relaxation agents (see Fig. 5). According to the present interpretation, the solvent accessibility could be measured directly in the EPR spectra, through the $2a_0$ parameter (Fig. 1 *a*), exploring the high sensitivity of the nitroxide to the solvent polarity. It is remarkable that all SC sulfhydryl groups accessed by the spin probes are localized in protein hydrophilic regions, as the isotropic hyperfine splitting ($2a_0$, Fig. 1 *a*) observed for the mobile component is the same as that of the spin label in buffer ($2a_0 = 34.2$ G, for hydrophobic environment this value can decrease to ~29 G). This also occurs for native sulfhydryl groups of other proteins, such as the membrane Na^+/K^+-ATPase from *Squalus accanthias* (Esmann et al., 1992), the membrane phosphate/H^+ translocator of rat liver mitochondria (Houstek et al., 1993), the creatine kinase (Liu and Zhou, 1995), and the membrane protein rhodopsin (Delmelle and Virmaux, 1977).

Effect of urea upon the mobility and conformational changes in SC protein

Urea causes drastic but completely reversible alterations in the SC proteins. At urea concentrations above 1 M an increase in the segmental motion of the backbone proteins was observed. Probably, urea expands the proteins opening the sulfhydryl pocket, reducing the cavity effects on the nitroxide inside the sulfhydryl groups (see Figs. 7 and 8 *B*). It has been shown that urea decreases the pressure that produces a given degree of virus dissociation, and this effect was interpreted as the progressive destabilization as a result of direct protein-urea interactions and not an indirect solvent effect (Weber et al., 1996). The dissociation of oligomeric proteins into subunits by hydrostatic pressure indicates that the separated solvated subunits occupy a smaller volume than the original aggregate (Silva and Weber, 1993; Weber et al., 1996). In the case of SC proteins urea caused

a great exposition of the SH groups to solvent, as can be observed by the large decrease in the pre-exponential factor of Eq. 2 (Fig. 7).

The studies showing that the naturally occurring solute, trimethylamine-*N*-oxide, counteracts the actions of urea on proteins are illustrative; small organic osmolytes, in many cases, have the property to protect intracellular proteins against its denaturation and loss of functional activity caused by urea (Mashino and Fridovich, 1987; Yancey and Somero, 1980; Baskakov et al., 1998). Mashino and Fridovich have proposed that urea loosens and expands protein volume, decreasing its functional activity, whereas trimethylamine-*N*-oxide would increase the protein activity by shifting its conformation toward the most compact and active form. Baskakov and co-workers (1998) have recently tested and found support for the above hypothesis for rabbit muscle lactate dehydrogenase function. These authors have pointed out that the effects of urea and trimethylamine-*N*-oxide are both related to the properties of these solutes on solvation. Thus, a poorer solvent than water, generally associated with organic compounds, will compete with water for the formation of hydrogen bonds with the protein, and favor more compact and less exposed protein conformations. Urea in aqueous solutions, being a better solvent than water in the sense that it can form hydrogen bonds with the protein enhancing the water protein hydration, will promote more expanded and exposed protein configurations. In SC, the activities of urea have been ascribed to its capacity of binding with proteins, causing swelling of the tissue and reducing the barrier property of the layer (Han et al., 1991). It is remarkable that urea, at 8 and 9.5 M plus a reducing agent, have been used to isolate keratins of the SC (Park et al., 1992; Eichner et al., 1992), showing its capacity to dissolve SC proteins.

To examine whether 8 M urea alters the SC-lipid dynamics we have spin-labeled the SC with the spin probes 5- and 16-doxylstearic acids (nitroxide at the 5th and 16th carbon atom positions of the acyl chain, respectively) as in previous work (Alonso et al., 2000a). Only very small alterations relative to the control samples were observed in the EPR spectra (not shown), except that for samples with urea a fraction of free spin labels systematically appears in the EPR spectra, indicating that urea creates domains of interstitial water in SC that are able to accommodate these hydrophobic nitroxides. Urea is considered a skin penetration enhancer for hydrophilic drugs, but when combined with alkanols or polyethylene glycol it can also accelerate permeation of lipophilic drugs such as progesterone and indomethacin (Valenta and Wedenig, 1997; Nishihata et al., 1990). Because urea does not significantly alter the order and mobility of the SC lipids, its action should be a result of the interactions with proteins. Treating the SC with the reducing agent dithiothreitol, Goates and Knutson (1993) have detected an increase in permeation for mannitol and sucrose in human epidermis. Because no significant alteration of lipid acyl chain mobility has been detected by infrared spectroscopy of SC in the presence of dithiothreitol, these data show strong evidence that polar solutes permeate the SC via pathways that involve the proteins.

In our early work (Alonso et al., 2000b) we analyzed the kinetics of maleimide spin-labeling of SC and it was observed that there are at least two non-equivalent SH groups in the SC. Of a total amount of ~4 nmol maleimide spin label/mg SC, about one-half reacted in the first hour of incubation and had an EPR signal similar to that analyzed here and for other native protein sulfhydryl groups reported in the literature for numerous systems. The other non-equivalent site can be accessed by blocking the first site with *N*-ethylmaleimide by 1 h of reaction followed by a subsequent 23-h additional incubation with the spin label. The EPR spectrum of this site shows a predominant contribution of component W, indicating that it is open and more exposed to the solvent. We have isolated the corneocyte envelope and the remaining proteins of SC (data not shown). From comparison of the EPR spectra of both samples it is clear that the proteins of the cell envelope provide the site that is spin-labeled first giving the two-component spectra described in this work and characteristic for maleimide spin-labeled proteins. The remaining proteins of SC (basically keratins) provide the other non-equivalent site (not studied here). This much less reactive site has a very different EPR signal and should be located predominantly inside the corneocyte. We would still like to mention that although the EPR signal with which we worked here was obtained from a variety of envelope proteins, it is very similar to those reported for other SH groups, as that of bovine serum albumin (Fig. 4). The basic difference between the EPR signals for albumin and for SC envelope proteins is associated with the largest mobility state of the polypeptide chains of albumin that is free to tumble in solution and has a higher state of hydration. The present work also shows a sensitive method to evaluate protein dynamics directly in the SC tissue by EPR spectroscopy, which may be useful to analyze different kinds of treatment effects on the SC and different cases of skin diseases.

We thank Prof. Dr. Fernando Pelegrini (Instituto de Física, Universidade Federal de Goiás) for his interest in this work. We thank Professors Richard H. Crepeau, Keith A. Earle, and Mingtao Ge for helping us to install the program NLLS.

This work was supported by Conselho Nacional de Desenvolvimento Científico e Tecnológico (CNP_q; grant process 300908/92-0), Fundação de Amparo à Pesquisa do Estado de São Paulo (FAPESP; processes 97/02431-4 and 95/6177-0), and Coordenação de Aperfeiçoamento de Pessoal de Nível Superior (CAPES).

REFERENCES

Abernethy, J. L., R. L. Hill, and L. A. Goldsmith. 1977. Epsilon-(gamma-glutamyl)lysine cross-links in human stratum corneum. *J. Biol. Chem.* 252:1837–1839.

Alonso, A., N. C. Meirelles, and M. Tabak. 1995. Effect of hydration upon the fluidity of intercellular membranes of stratum corneum: an EPR study. *Biochim. Biophys. Acta.* 1237:6–15.

Alonso, A., N. C. Meirelles, and M. Tabak. 2000a. Lipid chain dynamics in stratum corneum studied by spin label electron paramagnetic resonance. *Chem. Phys. Lipids.* 104:101–111.

Alonso, A., N. C. Meirelles, V. E. Yushmanov, and M. Tabak. 1996. Water increases the fluidity of intercellular membranes of stratum corneum: correlation with water permeability, elastic, and electrical properties. *J. Invest. Dermatol.* 106:1058–1063.

Alonso, A., J. G. Santos, and M. Tabak. 2000b. Stratum corneum protein mobility as evaluated by a spin label maleimide derivative. *Biochim. Biophys. Acta.* 1478:89–101.

Barnes, J. P., Z. Liang, H. S. Mchaourab, J. H. Freed, and W. L. Hubbell. 1999. A multifrequency electron spin resonance study of T4 lysozyme dynamics. *Biophys. J.* 76:3298–3306.

Baskakov, I., A. Wang, and D. W. Bolen. 1998. Trimethylamine-*N*-oxide counteracts urea effects on rabbit muscle lactate dehydrogenase function: a test of the counteraction hypothesis. *Biophys. J.* 74:2666–2673.

Behne, M., Y. Uchida, T. Seki, P. O. Montellano, P. M. Elias, and W. M. Holleran. 2000. Omega-hydroxyceramides are required for corneocyte lipid envelope (CLE) formation and normal epidermal permeability barrier function. *J. Invest. Dermatol.* 114:185–192.

Blank, I. H., J. Moloney, A. G. Emslie, I. Simon, and C. Apt. 1984. The diffusion of water across the stratum corneum as a function of its water content. *J. Invest. Dermatol.* 82:188–194.

Breathnach, A. S., T. Goodman, C. Stolinski, and M. Gross. 1973. Freeze fracture replication of cells of stratum corneum of human epidermis. *J. Anat.* 114:65–81.

Budil, D. E., S. Lee, S. Saxena, and J. H. Freed. 1996. Nonlinear-least-squares analysis of slow-motional EPR spectra in one and two dimensions using a modified Levenberg-Marquardt algorithm. *J. Magn. Reson. A.* 120:155–189.

Delmelle, M. N., and N. Virmaux. 1977. Location of two sulfhydryl groups in the rhodopsin molecule by use of the spin label technique. *Biochim. Biophys. Acta.* 464:370–377.

Downing, D. T. 1992. Lipid and protein structures in the permeability barrier of mammalian epidermis. *J. Lipid Res.* 33:301–313.

Eichner, R., M. Kahn, R. J. Capetola, G. J. Gendimenico, and J. A. Mezick. 1992. Effects of topical retinoids on cytoskeletal proteins: implications for retinoid effects on epidermal differentiation. *J. Invest. Dermatol.* 98:154–161.

El-Shime, A. F., and H. M. Princen. 1978. Diffusion characteristics of water vapor in some keratins. *Colloid Polymers Sci.* 256:209–217.

Esmann, M., H. O. Hankovszky, K. Hideg, and D. Marsh. 1989. A novel spin-label for study of membrane protein rotational diffusion using saturation transfer electron spin resonance. Application to selectively labeled class I and class II -SH groups of the shark rectal gland Na^+/K^+-ATPase. *Biochim. Biophys. Acta.* 978:209–215.

Esmann, M., K. Hideg, and D. Marsh. 1992. Conventional and saturation transfer EPR spectroscopy of Na^+/K^+-ATPase modified with different maleimide-nitroxide derivatives. *Biochim. Biophys. Acta.* 1159:51–59.

Esmann, M., L. I. Horváth, and D. Marsh. 1987. Saturation-transfer electron spin resonance studies on the mobility of spin-labeled sodium and potassium ion activated adenosinetriphosphatase in membranes from *Squalus acanthias*. *Biochemistry.* 26:8675–8683.

Goates, C. Y., and K. Knutson. 1993. Enhanced permeation and stratum corneum structural alterations in the presence of dithiothreitol. *Biochim. Biophys. Acta.* 1153:289–298.

Goldsmith, L. A., H. P. Baden, S. I. Roth, R. Colman, L. Lee, and B. Fleming. 1974. Vertebral epidermal transamidases. *Biochim. Biophys. Acta.* 351:113–125.

Gray, G. M., R. J. White, and H. J. Yardley. 1982. Lipid composition of the superficial stratum corneum cells of the epidermis. *Br. J. Dermatol.* 106:59–63.

Griffith, O. H., and P. C. Jost. 1976. Lipid spin labels in biological membranes. *In* Spin Labeling. Theory and Applications. L. J. Berliner, editor. Academic Press, New York. 453–523.

Han, S. K., Y. H. Jun, Y. J. Rho, S. C. Hong, and Y. M. Kim. 1991. Percutaneous absorption-enhancing activity of urea derivatives. *Arch. Pharm. Res.* 14:112–118.

Hohl, D. 1990. Cornified cell envelope. *Dermatologica.* 180:201–221.

Houstek, J., E. Bertoli, I. Stipani, S. Pavelka, F. M. Megli, and F. Palmieri. 1993. Characterization of sulfhydryl groups of the mitochondrial phosphate translocator by a maleimide spin label. *FEBS Lett.* 154:185–190.

Lai, C. S., N. M. Tooney, and E. G. Ankel. 1984. Spin label studies of sulfhydryl environment in plasma fibronectin. *FEBS Lett.* 173:283–286.

Liang, Z., J. H. Freed, R. S. Keyes, and A. M. Bobst. 2000. An electron spin resonance study of DNA dynamics using the slowly relaxing local structure model. *J. Phys. Chem. B.* 104:5372–5381.

Liu, Z. J., and J. M. Zhou. 1995. Spin-labeling probe on conformational change at the active sites of creatine kinase during denaturation by guanidine hydrochloride. *Biochim. Biophys. Acta.* 1253:63–68.

Mashino, T., and I. Fridovich. 1987. Effects of urea and trimethylamine-*N*-oxide on enzyme activity and stability. *Arch. Biochem. Biophys.* 258:356–360.

Matoltsy, A. G., and M. N. Matoltsy. 1970. The chemical nature of keratohyalin granules of the epidermis. *J. Cell Biol.* 47:593–603.

Mchaourab, H. S., T. Kálai, K. Hideg, and W. L. Hubbell. 1999. Motion of spin-labeled side chains in T4 lysozyme: effect of side chain structure. *Biochemistry* 38:2947–2955.

Mchaourab, H. S., M. A. Lietzow, K. Hideg, and W. L. Hubbell. 1996. Motion of spin-labeled side chains in T4 lysozyme: correlation with protein structure and dynamics. *Biochemistry.* 35:7692–7704.

Nemes, Z., L. N. Marekov, L. Fésüs, and P. M. Steinert. 1999. A novel function for transglutaminase 1: attachment of long-chain omega-hydroxyceramides to involucrin by ester bond formation. *Proc. Natl. Acad. Sci. U.S.A.* 96:8402–8407.

Nishihata, T., J. H. Rytting, A. Kamada, K. Matsumoto, and K. Takahashi. 1990. Combined effect of alcohol and urea on the in vitro transport of indomethacin across rat dorsal skin. *J. Pharm. Sci.* 79:487–489.

Öhman, H., and A. Vahlquist. 1998. The pH over the stratum corneum differs in x-linked recessive and autosomal dominant ichthyosis: a clue to the molecular origin of the "acid skin mantle"? *J. Invest. Dermatol.* 111:674–677.

Park, J. K., T. Yoshiike, H. Yaguchi, and H. Ogawa. 1992. Isolation and characterization of a lower molecular weight protein doublet of horny cell outer leaflet: a possible novel epidermal differentiation marker. *Br. J. Dermatol.* 127:372–378.

Rice, R. H., and H. Green. 1977. The cornified envelope of terminally differentiated human epidermal keratinocytes consists of cross-linked protein. *Cell.* 11:417–422.

Russell, C. J., T. E. Thorgeirsson, and Y. K. Shin. 1999. The membrane affinities of the aliphatic amino acid side chains in an α-helical context are independent of membrane immersion depth. *Biochemistry.* 38:337–346.

Sankarapandi, S., D. A. Walz, R. S. Zafar, and L. J. Berliner. 1995. Electron spin resonance and fluorescence studies of the conformational environment of the thiol groups of thrombospondin: interactions with thrombin. *Biochemistry.* 34:10491–10496.

Schneider, D. J., and J. H. Freed. 1989. Calculating slow motional magnetic resonance spectra: a user's guide. *In* Biological Magnetic Resonance, Vol. 8. L. J. Berliner and J. Reuben, editors. Plenum Press, New York. 1–76.

Silva, J. L., and G. Weber. 1993. Pressure stability of proteins. *Annu. Rev. Phys. Chem.* 44:89–113.

Steinert, P. M., and L. N. Marekov. 1995. The proteins elafin, filagrin, keratin intermediate filaments, loricrin, and small proline-rich proteins 1 and 2 are isodipeptide cross-linked components of the human epidermal cornified cell envelope. *J. Biol. Chem.* 270:17702–17711.

Steinert, P. M., and L. N. Marekov. 1999. Initiation of assembly of the cell envelope barrier structure of stratified squamous epithelia. *Mol. Biol. Cell.* 10:4247–4261.

Steven, A. C., and P. M. Steinert. 1994. Protein composition of cornified cell envelopes of epidermal keratinocytes. *J. Cell Sci.* 107:693–700.

Swartzendruber, D. C., P. W. Wertz, D. J. Kitko, K. C. Madison, and D. T. Downing. 1989. Molecular models of the intercellular lipid lamellae in mammalian stratum corneum. *J. Invest. Dermatol.* 92:251–257.

Valenta, C., and S. Wedenig. 1997. Effects of penetration enhancers on the in vitro percutaneous absorption of progesterone. *J. Pharm. Pharmacol.* 49:955–959.

Weber, G., A. T. Da Poian, and J. L. Silva. 1996. Concentration dependence of the subunit association of oligomers and viruses and the modification of the latter by urea binding. *Biophys. J.* 70:167–173.

Wertz, P. W., and D. T. Downing. 1987. Covalently bound ω-hydroxyacylsphingosine in the stratum corneum. *Biochim. Biophys. Acta.* 917: 108–111.

Wertz, P. W., D. C. Swartzendruber, D. J. Kitko, K. C. Madison, and D. T. Downing. 1989. The role of the corneocyte lipid envelopes in cohesion of the stratum corneum. *J. Invest. Dermatol.* 93:169–172.

Yancey, P. H., and G. N. Somero. 1980. Methylamine osmoregulatory solutes of elasmogranch fishes counteract urea inhibition of enzymes. *J. Exp. Zool.* 212:205–213.

Zhan, H., O. J. Kyoung, Y. K. Shin, W. L. Hubbell, and R. J. Collier. 1995. Interaction of the isolated transmembrane domain of diphtheria toxin with membranes. *Biochemistry.* 34:4856–4863.